NATIONAL AERONAUTICS AND SPACE ADMINISTRATION

Technical Report 32-1158

Stiffness Matrix for a Triangular Sandwich Element in Bending

H. C. Martin

JET PROPULSION LABORATORY

CALIFORNIA INSTITUTE OF TECHNOLOGY

PASADENA, CALIFORNIA

October 1, 1967

NATIONAL AERONAUTICS AND SPACE ADMINISTRATION

Technical Report 32-1158

Stiffness Matrix for a Triangular Sandwich Element in Bending

H. C. Martin

Approved by:

M. E. Alper

M. E. Alper, Manager
Applied Mechanics Section

JET PROPULSION LABORATORY

CALIFORNIA INSTITUTE OF TECHNOLOGY

PASADENA, CALIFORNIA

October 1, 1967

TECHNICAL REPORT 32-1158

Preface

This report is a summary of research conducted by the author as a consultant to the Jet Propulsion Laboratory. The work was originally prepared in 1964–65 and was subsequently extended in 1967. The author is Professor of Aeronautics and Astronautics at the University of Washington, Seattle, Washington.

Acknowledgement

Contents

Contents (contd)

Contents (contd)

Figures (contd)

Abstract

The finite element presented in this report is useful for analyzing plates and shells by the direct stiffness method. Both conventional thin plates and shells, as well as sandwich structures, are included. The stiffness matrix derivation is both simple and straightforward, since it is based on previously published material. A few examples are included to illustrate the accuracy obtained with this element.

Stiffness Matrix for a Triangular Sandwich
Element in Bending

I. Introduction

This report presents various phases of the development of a triangular finite element in bending. A sandwich element is chosen because it provides the simplest basis for obtaining a satisfactory stiffness matrix. At the same time, the sandwich element is applicable to sandwich panels, as well as to conventional thin plates and shells.

The triangular element stiffness matrix, plus the numerical proceedings of the stiffness method, yields deflections and stresses for the most general classes of plate and shell problems. Although results will be approximate, experience has shown that they are usually adequate for engineering design purposes.

Interest in the triangular element in bending during the late 1950's, led to work directed toward finding a suitable stiffness matrix. These efforts proceeded along two totally different paths. The first considered the element as a typical thin-plate unit. By choosing a deflection function, $w(x, y)$, straightforward concepts of the stiffness method could be followed in deriving the element stiffness matrix. References 1–4 give examples of this early work. Results were generally unsatisfactory and could not be used in engineering design. The difficulty resided in the selection of a satisfactory deflection function.

At about the same time, R. J. Melosh, then at The Boeing Company, recognized that a second path was available. The stiffness matrix for the triangle in plane stress was already known (Ref. 5). Hence, it was decided to use these parts as the cover sheets of a sandwich element and, on that basis, obtain a stiffness matrix for the triangle in bending. Melosh (Ref. 6) in his paper states that "publication was delayed due to dissatisfaction with the derivation in its initial form." Nevertheless, a correct result for the sandwich element had been found. This led to satisfactory data when applied to plate and shell problems. Reference 7 gives a number of examples, the solutions to some of which were reached by using the original stiffness matrix obtained for the triangular sandwich element.

In the meantime, it has been recognized that the triangular element in bending presents difficulties which had not been encountered in the initial work on finite elements. By adopting the standard procedure of simply considering nodes to exist at the three vertices of the triangle, it was eventually realized that a satisfactory function $w(x, y)$ could not be established. Fraeijs de Veubeke first suggested the need for introducing additional nodes in such cases, and this led to the so-called HCT (Hsieh, Clough, Tocher) triangle as presented by Clough and Tocher in Ref. 8. By introducing an additional node at

the centroid of the triangle, it became possible to replace the original area with three subtriangles. This, in turn, permitted much greater generality to be exercised in forming $w (x, y)$. Clough and Tocher show in Ref. 8 that, on this basis, a greatly improved bending stiffness matrix for the conventional triangle in bending could be derived.

The sandwich element discussed in this report leads to the same stiffness matrix obtainable from Ref. 6. The same element is used in the COSMOS program at The Boeing Company and in the SAMIS program developed at the Jet Propulsion Laboratory. However, the derivation is entirely different from that given in Ref. 6. The development of the stiffness matrix proceeds in a straightforward manner if based on a clear statement as to the nature of the element. An explicit final form is obtained for the stiffness matrix. This, in turn, proves to be useful for looking into certain questions arising with respect to this element.

It is important to recognize that the sandwich-type element enjoys some unique characteristics which make it useful to the structural designer. Among these are:

1. Orthotropic, or even aeolotropic, material properties may be represented. Furthermore, these properties need not be the same for cover sheets and connecting shear core.

2. Design orthotropy, as illustrated by corrugation or stiffeners held between cover sheets, may also be represented by this element.

3. Plate or shell sections having appreciable shear flexibility are reasonably idealized by the sandwich element.

4. Structures containing plates or shells, reinforced with beams or frames, present idealization problems. In general, finite plate and beam elements will not remain compatible along common edges as deflec-

tion takes place. Since the sandwich plate and beam elements do not undergo curvature, the opportunity for achieving such compatibility is greatly enhanced if the sandwich elements are used.

5. The triangular sandwich element preserves both displacement and "slope" continuity across edges common to adjacent triangles. Furthermore, this is true even when the triangles lie in different planes, as when used to represent a curved shell.

6. Since this element remains flat when representing plate or shell bending, it may be used with the initial stress stiffness matrix developed by the author (Ref. 9) to represent large deflection and stability behavior.

II. The Isotopic Triangle in Bending

A. Sandwich Element—Description

The triangular element presented herein is visualized as consisting of identical top and bottom cover sheets, separated by thin shear webs located at each edge of the triangle (Fig. 1).

To specify the element, it is necessary to give its overall thickness d, cover sheet thickness h, and shear web thickness t_w, as well as E, G, and v, in terms of the actual plate. The basis for doing this will be taken up prior to deriving the element stiffness matrix.

Bending moments are resisted solely by the cover sheets. These plane stress members are restricted to a constant state of strain. As such, their stiffness matrix is given by Eq.(B-3), Ref. 5. Shear webs transmit the transverse loading. Each is assumed to be in a state of pure shear. As such, their stiffness matrix is given by Eq. (4.85), Ref. 10. The stiffness matrix for the total element will be developed by using these component stiffness matrices.
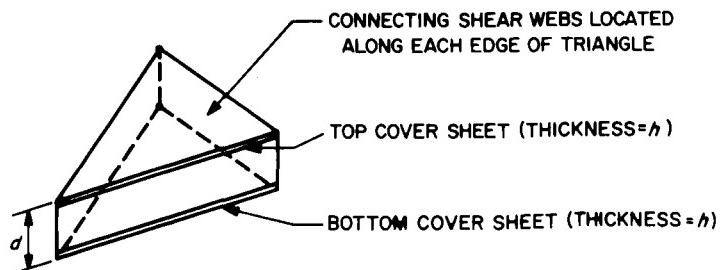

Fig. 1. Component parts of the triangular sandwich element

The corresponding sandwich beam element is discussed in Ref. 10. Reference 10 also shows how well such an element will predict actual beam behavior. Both the beam and triangular elements remain flat as they deform under loading. Nevertheless, the ability of the sandwich element to predict beam behavior provides encouragement for extending this concept to the more complex case of the triangle.

It should be kept in mind that the top and bottom covers are strained asymmetrically. For the beam element this means that, if the upper flange is in compression, the lower flange will experience an equal tensile strain.

B. Sandwich Element—Properties

1. Displacements and forces. If it is assumed that the element lies in the xy plane, then displacements u and v at each node define the deformation in the cover sheets. Normal displacements w define the shear web deformation at each node. It will be convenient to replace u and v by slopes θ_x and θ_y for the complete element. Consequently, three nodal displacements exist at each node, leading to a 9×9 stiffness matrix for the element. A sketch of the element is shown in Fig. 2a. The middle plane is shown in Fig. 2b.
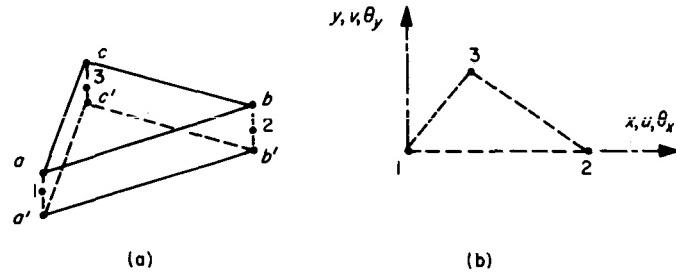
Fig. 2. Nodal representation for the sandwich element

Asymmetrical behavior of the top and bottom cover sheets are defined by

$$u_\alpha = - u_{\alpha'} \qquad v_\alpha = - v_{\alpha'} \qquad (1a)$$

and

$$w_\alpha = w_{\alpha'} = w_i \qquad (1b)$$

where

$$\alpha = a, b, c$$

and

$$i = 1, 2, 3$$

The slopes may be introduced in place of u and v by referring to Fig. 3 which demonstrates that the following equations apply:

$$\theta_{x_1} = - \frac{v_a}{d/2} , \qquad \theta_{y_1} = \frac{u_a}{d/2} \qquad (2)$$
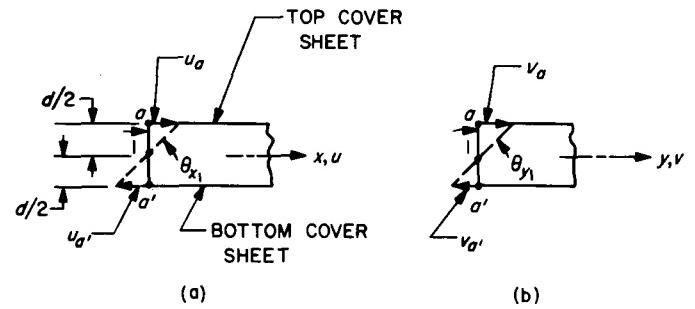
Fig. 3. Relation between cover sheet displacements (u, v) and corresponding sandwich element displacements (θ_x, θ_y)

The signs in Eq. (2) follow from Fig. 2b and Figs. 3a and 3b.

Writing Eq. (2) at all nodes and collecting results gives

$$
\begin{Bmatrix} u_a \\ v_a \\ u_b \\ v_b \\ u_c \\ v_c \end{Bmatrix}
= \frac{d}{2}
\begin{bmatrix}
0 & 1 & & & & \\
-1 & 0 & & & & \\
& & 0 & 1 & & \\
& & -1 & 0 & & \\
& & & & 0 & 1 \\
& & & & -1 & 0
\end{bmatrix}
\begin{Bmatrix} \theta_{x_1} \\ \theta_{y_1} \\ \theta_{x_2} \\ \theta_{y_2} \\ \theta_{x_3} \\ \theta_{y_3} \end{Bmatrix}
$$

$$(3a)$$

or simply

$$\mathbf{u} = \frac{d}{2} \mathbf{T} \boldsymbol{\theta} \qquad (3b)$$

Note: Boldface symbols represent matrices.

All elements not shown in **T**, Eqs. (3a) and (3b), are zero.

Cover sheets carry in-plane stresses σ_x, σ_y, and τ_{xy}. In deriving the cover sheet stiffness matrix these stresses are replaced by equivalent nodal forces, X_α and Y_α. Figure 4 illustrates these nodal forces.
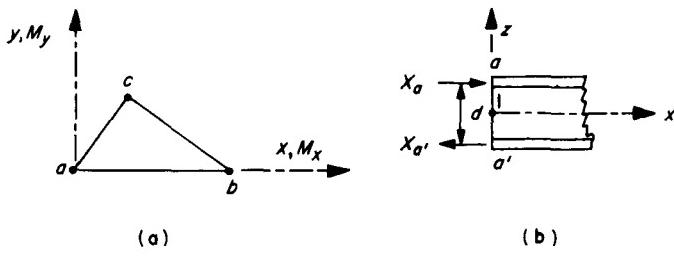
Fig. 4. Nodal forces for cover sheets

The following relations for the forces are in harmony with Eqs. (1a) and (1b) for displacements.

$$X_a = - X_{a'}$$

$$Y_a = - Y_{a'} \tag{4a}$$

and

$$Z_a = Z_{a'} = Z_1/2 \tag{4b}$$

The moments applicable to the sandwich element are then

$$M_{x_1} = - Y_a d \quad , \quad M_{y_1} = X_a d \tag{5}$$

Again, writing the last equations for each node and collecting results

$$
\begin{Bmatrix} M_{x_1} \\ M_{y_1} \\ \hline M_{x_2} \\ M_{y_2} \\ \hline M_{x_3} \\ M_{y_3} \end{Bmatrix}
= d
\begin{bmatrix}
0 & -1 & & & & \\
1 & 0 & & & & \\
\hline
& & 0 & -1 & & \\
& & 1 & 0 & & \\
\hline
& & & & 0 & -1 \\
& & & & 1 & 0
\end{bmatrix}
\begin{Bmatrix} X_a \\ Y_a \\ \hline X_b \\ Y_b \\ \hline X_c \\ Y_c \end{Bmatrix}
\tag{6a}
$$

where elements not shown in the square matrix of Eq. (6a) are again to be taken as zero. Comparing Eq. (6a) with Eq. (3) leads to

$$\mathbf{M} = d\, \mathbf{T}^T \mathbf{X} \tag{6b}$$

where $\mathbf{T}^T$ is the transpose of $\mathbf{T}$.

2. Cover sheet thickness. The cover sheet thickness is established by requiring a unit width of the sandwich panel to have the same moment of inertia as a unit width of the true plate. Or, from Fig. 5

$$I \text{ (sandwich)} = I \text{ (actual structure)}$$

$$2h \left(\frac{d}{2}\right)^2 = \frac{t^3}{12}$$

In the last equation the thickness, d, of the sandwich may be selected arbitrarily. For convenience, put

$$d = t \tag{7a}$$

Then

$$h = \frac{t}{6} \tag{7b}$$

Equations (7a) and (7b) define the sandwich element cover sheets in terms of the actual structure plate thickness.
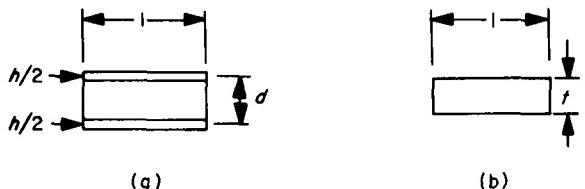
Fig. 5. Unit strips of sandwich and solid plates

3. Shear web thicknesses. The depth of the shear web is t, as given by Eq. (7a). To determine the appropriate thickness for the shear webs, both the solid triangle and the corresponding sandwich element will be subjected to pure shearing displacement modes. The sandwich element will then be required to develop the same energy as the solid triangle. One such mode is represented by $w_1 \neq 0$, while all other nodal displacements are zero. This mode is shown in Fig. 6.
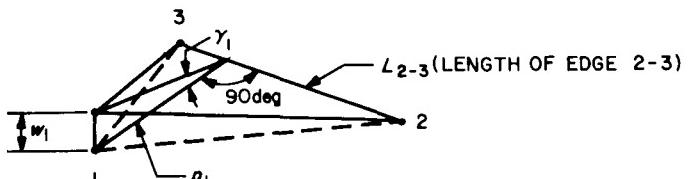
Fig. 6. Pure shearing displacement mode

If Fig. 6 is initially assumed to represent shearing of the true, solid element, the shear strain γ_1 may be written as

$$\gamma_1 = \frac{w_1}{P_1}$$

Hence

$$\gamma_1 = \frac{L_{2-3}}{2A} w_1$$

where

$$A = P_1 L_{2-3}/2 = \text{area of triangle}$$

Strain energy $U_I^{(1)}$ associated with this deformation may then be written as

$$U_I^{(1)} = \frac{1}{2} \int \int \int \tau \, \gamma_1 \, dx \, dy \, dz$$

where

$$\tau = G \gamma_1$$

Hence

$$U_I^{(1)} = \frac{Gt \, L_{2-3}^2}{8} w_1^2$$

Repeating for the two additional shearing modes and superimposing gives the total strain energy U_I for the solid plate as

$$U_I = \frac{Gt}{8A} (L_{1-2}^2 \, w_3^2 + L_{2-3}^2 \, w_1^2 + L_{3-1}^2 \, w_2^2) \tag{8}$$

Next, assume Fig. 6 to represent the sandwich element. Shear webs located along edges 1-2 and 1-3 are strained in this mode. In this case, the respective shear strains are

$$\gamma_1 = \frac{w_1}{L_{1-2}} \qquad \gamma_2 = \frac{w_2}{L_{1-3}}$$

Corresponding strain energy $U_{II}^{(1)}$ then takes the form

$$U_{II}^{(1)} = \frac{G}{2}\left[\left(\frac{A_w}{L}\right)_{1-2} + \left(\frac{A_w}{L}\right)_{1-3}\right] w_1^2$$

where A_w is the shear web cross-sectional area. Repeating this calculation for the other two modes and superimposing gives the total energy U_{II} as

$$U_{II} = \frac{G}{2} \left\{ \left[\left(\frac{A_w}{L}\right)_{1-2} + \left(\frac{A_w}{L}\right)_{1-3}\right] w_1^2 + \left[\left(\frac{A_w}{L}\right)_{1-2} \right. \right.$$
$$\left. \left. + \left(\frac{A_w}{L}\right)_{2-3}\right] w_2^2 + \left[\left(\frac{A_w}{L}\right)_{1-3} + \left(\frac{A_w}{L}\right)_{2-3}\right] w_3^2 \right\} \tag{9}$$

Strain energies U_I and U_{II} can now be made equal to each other by requiring the coefficients of the squares of the displacements to be equal. Doing this and solving for shear web areas gives

$$\left\{ \begin{array}{c} \left(\dfrac{A_w}{L}\right)_{1-2} \\[1em] \left(\dfrac{A_w}{L}\right)_{2-3} \\[1em] \left(\dfrac{A_w}{L}\right)_{3-1} \end{array} \right\} = \frac{t}{8A} \begin{bmatrix} -1 & 1 & 1 \\ 1 & -1 & 1 \\ 1 & 1 & -1 \end{bmatrix} \left\{ \begin{array}{c} L_{1-2}^2 \\[1em] L_{2-3}^2 \\[1em] L_{3-1}^2 \end{array} \right\} \tag{10}$$

Equation (10) specifies the shear web cross-sectional areas. The sandwich element is now completely defined such that it will represent the actual thin plate which it is intended to represent.

C. Stiffness Due to Cover Sheets

The cover sheet stiffness matrix of Eq. (B-3), Ref. 5, relates X_α, Y_α nodal forces to the corresponding u_α, v_α nodal displacements. For the top cover, the stiffness equation may be expressed as

$$\left\{ \begin{array}{c} X_a \\ Y_a \\ \hline X_b \\ Y_b \\ \hline X_c \\ Y_c \end{array} \right\} = \mathbf{K}_{cs} \left\{ \begin{array}{c} u_a \\ v_a \\ \hline u_b \\ v_b \\ \hline u_c \\ v_c \end{array} \right\} \tag{11a}$$

or

$$\mathbf{X} = \mathbf{K}_{cs} \, \mathbf{u} \tag{11b}$$

where, from Ref. 5

$$\mathbf{K}_{cs} = \frac{Eh\phi}{2}\begin{bmatrix}
\lambda_1 x_{23}^2 + y_{23}^2 & & & & \text{(SYMMETRIC)} & \\
\lambda_2 x_{32} y_{23} & x_{23}^2 + \lambda_1 y_{23}^2 & & & & \\
\lambda_1 x_{23} x_{31} + y_{23} y_{31} & \lambda_1 x_{13} y_{23} + \nu x_{23} y_{13} & \lambda_1 x_{13}^2 + y_{13}^2 & & & \\
\lambda_1 x_{23} y_{13} + \nu x_{13} y_{23} & x_{23} x_{31} + \lambda_1 y_{23} x_{31} & \lambda_2 x_{13} y_{31} & x_{13}^2 + \lambda_1 y_{13}^2 & & \\
\lambda_1 x_{12} x_{23} + y_{12} y_{23} & \lambda_1 x_{21} y_{23} + \nu x_{32} y_{12} & \lambda_1 x_{12} x_{31} + y_{12} y_{31} & \lambda_1 x_{12} y_{13} + \nu x_{13} y_{12} & \lambda_1 x_{12}^2 + y_{12}^2 & \\
\lambda_1 x_{32} y_{12} + \nu x_{21} x_{23} & x_{12} x_{23} + \lambda_1 y_{12} y_{23} & \lambda_1 x_{13} y_{12} + \nu x_{12} y_{13} & x_{12} x_{31} + \lambda_1 y_{12} y_{31} & \lambda_2 x_{21} y_{12} & x_{12}^2 + \lambda_1 y_{12}^2
\end{bmatrix}$$

<div align="right">

column headers: $u_a \quad v_a \quad u_b \quad v_b \quad u_c \quad v_c$

</div>

in which $\qquad\qquad\qquad\qquad\qquad\qquad\qquad\qquad\qquad\qquad\qquad$ (11c)

$$x_{\alpha\beta} = x_\alpha - x_\beta, \text{ etc.}$$

$$\phi = \frac{1}{2(1 - \nu^2) A}$$

where

$A = $ area of triangle

$\nu = $ Poisson's ratio

$$\lambda_1 = \frac{1 - \nu}{2}$$

$$\lambda_2 = \frac{1 + \nu}{2}$$

Also, it should be remembered that, in Ref. 5, the sheet thickness is represented by t, while in this report, h is used for cover sheet thickness and t for the total element thickness.

The forces and displacements of Eqs. (11a), (11b), (11c) must now be rewritten in terms of moments and slopes. This is easily done by substituting Eq. (3b) into Eq. (11b), and the result into Eq. (6b)

$$\mathbf{M} = \frac{t^2}{2} (\mathbf{T}^T \mathbf{K}_{cs} \mathbf{T}) \, \boldsymbol{\theta} \qquad (12a)$$

Therefore, the bending portion of the sandwich element stiffness matrix is

$$\mathbf{K}_b = \frac{t^2}{2} (\mathbf{T}^T \mathbf{K}_{cs} \mathbf{T}) \qquad (12b)$$

Carrying out the triple matrix product and using Eqs. (7a) and (7b) leads to

$$\mathbf{K}_b = \frac{Et^3\phi}{24}\begin{bmatrix}
x_{23}^2 + \lambda_1 y_{23}^2 & & & & \text{(SYMMETRIC)} & \\
-\lambda_2 x_{32} y_{23} & \lambda_1 x_{23}^2 + y_{23}^2 & & & & \\
x_{23} x_{31} + \lambda_1 y_{23} y_{31} & -\lambda_1 x_{23} y_{13} - \nu x_{13} y_{23} & x_{13}^2 + \lambda_1 y_{13}^2 & & & \\
-\lambda_1 x_{13} y_{23} - \nu x_{23} y_{13} & \lambda_1 x_{23} x_{31} + y_{23} y_{31} & -\lambda_2 x_{13} y_{31} & \lambda_1 x_{13}^2 + y_{13}^2 & & \\
x_{12} x_{23} + \lambda_1 y_{12} y_{23} & -\lambda_1 x_{32} y_{12} - \nu x_{21} y_{23} & x_{12} x_{31} + \lambda_1 y_{12} y_{31} & -\lambda_1 x_{13} y_{12} - \nu x_{12} y_{13} & x_{12}^2 + \lambda_1 y_{12}^2 & \\
-\lambda_1 x_{21} y_{23} - \nu x_{32} y_{12} & \lambda_1 x_{12} x_{23} + y_{12} y_{23} & -\lambda_1 x_{12} y_{13} - \nu x_{13} y_{12} & \lambda_1 x_{12} x_{31} + y_{12} y_{31} & -\lambda_2 x_{21} y_{12} & \lambda_1 x_{12}^2 + y_{12}^2
\end{bmatrix}$$

<div align="right">

column headers: $\theta_{x_1} \quad \theta_{y_1} \quad \theta_{x_2} \quad \theta_{y_2} \quad \theta_{x_3} \quad \theta_{y_3}$

</div>

$$\qquad\qquad\qquad\qquad\qquad\qquad\qquad\qquad\qquad\qquad\qquad \text{(12c)}$$

For the sandwich beam element, the corresponding flange member stiffness matrix can be found from the discussion given in Ref. 10.

D. Stiffness Due to Shear Webs

It is convenient to begin the discussion by considering shear web 1-2 located along the x-axis (Figs. 2 and 7). Equation (4.85), Ref. 10, gives the appropriate stiffness matrix for this member. Forces X_a, X_b, etc., are from the cover sheets in the case of the sandwich triangular element. Equations (4a) and (4b) apply to the forces shown in Fig. 7.

$$
\left\{\begin{array}{c} X_a \\ Z_a \\ X_b \\ Z_b \end{array}\right\} = \frac{G(A_w)_{1-2}}{2t} \begin{bmatrix} \dfrac{L_{1-2}}{t} & & \text{(SYMMETRIC)} \\ -1 & \dfrac{t}{L_{1-2}} & & \\ \dfrac{L_{1-2}}{t} & -1 & \dfrac{L_{1-2}}{t} & \\ 1 & -\dfrac{t}{L_{1-2}} & 1 & \dfrac{t}{L_{1-2}} \end{bmatrix} \left\{\begin{array}{c} u_a \\ w_a \\ u_b \\ w_b \end{array}\right\}
$$

(13a)

or

$$\overline{X} = (\overline{K}_w)_{1-2}\,\overline{u} \tag{13b}$$

where $(A_w)_{1-2}$ is the cross-sectional area of the shear web and the bars over the symbols in Eq. (13b) indicate that the member lies along the x-axis.

The first step is to transform Eq. (13) such that the member may lie at an angle Ψ to the x-axis. Such transformations are discussed in detail in Ref. 10. The appropriate transformation equations are

$$X = \Lambda^T \overline{X} \quad \text{and} \quad \overline{u} = \Lambda u \tag{14a}$$

where

$$
\Lambda = \begin{bmatrix} \lambda & \mu & 0 & 0 & 0 & 0 \\ -\mu & \lambda & 0 & 0 & 0 & 0 \\ 0 & 0 & 1 & 0 & 0 & 0 \\ 0 & 0 & 0 & \lambda & \mu & 0 \\ 0 & 0 & 0 & -\mu & \lambda & 0 \\ 0 & 0 & 0 & 0 & 0 & 1 \end{bmatrix} \tag{14b}
$$

and

$$\lambda = \cos\Psi \quad , \quad \mu = \sin\Psi \tag{14c}$$

It should be noted that, in writing Λ, Eq. (13a) has been rewritten to include Y_a and $Y_{a'}$ and v_a, $v_{a'}$. This requires
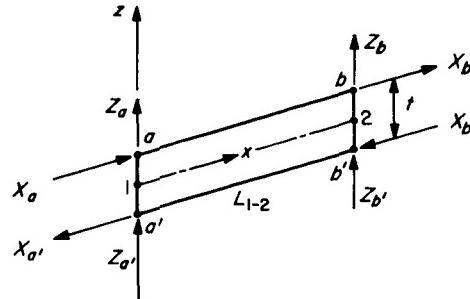
rows and corresponding columns of zeros to be included in $(\overline{K}_w)_{1-2}$. This generalization of the equation does not alter the basic content of Eq. (13a). Substituting Eq. (13b) and the second part of Eq. (14a) into the first part of Eq. (14a) gives

$$
\begin{aligned}
X &= \Lambda^T (\overline{K}_w)_{1-2} \Lambda u \\
&= (\hat{K}_w)_{1-2}\, u
\end{aligned} \tag{15a}
$$

Equation (15a) must now be transformed into moments and slopes consistent with the terms used for the cover sheets. At the same time, Z_a of Eq. (13a) should be replaced by Z_1 (Eq. 4b). Using Eqs. (6a) and (7a), the forces of Eq. (15a) may be related to moments as follows (with $Z_1 = 2Z_a$):

$$
\left\{\begin{array}{c} M_{x_1} \\ M_{y_1} \\ Z_1 \\ M_{x_2} \\ M_{y_2} \\ Z_2 \end{array}\right\} = \begin{bmatrix} 0 & -t & 0 & 0 & 0 & 0 \\ t & 0 & 0 & 0 & 0 & 0 \\ 0 & 0 & 2 & 0 & 0 & 0 \\ 0 & 0 & 0 & 0 & -t & 0 \\ 0 & 0 & 0 & t & 0 & 0 \\ 0 & 0 & 0 & 0 & 0 & 2 \end{bmatrix} \left\{\begin{array}{c} X_a \\ Y_a \\ Z_a \\ X_b \\ Y_b \\ Z_b \end{array}\right\}
$$

(15b)

By similarly treating displacements (Eq. 3a)

$$
\left\{\begin{array}{c} u_1 \\ v_1 \\ w_1 \\ u_2 \\ v_2 \\ w_2 \end{array}\right\} = \begin{bmatrix} 0 & t/2 & 0 & 0 & 0 & 0 \\ -t/2 & 0 & 0 & 0 & 0 & 0 \\ 0 & 0 & 1 & 0 & 0 & 0 \\ 0 & 0 & 0 & 0 & t/2 & 0 \\ 0 & 0 & 0 & -t/2 & 0 & 0 \\ 0 & 0 & 0 & 0 & 0 & 1 \end{bmatrix} \left\{\begin{array}{c} \theta_{x_1} \\ \theta_{y_1} \\ w_1 \\ \theta_{x_2} \\ \theta_{y_2} \\ w_2 \end{array}\right\}
$$

(15c)

Now, by substituting Eq. (15c) into (15a) and the result into Eq. (15b)

$$
\begin{Bmatrix} M_{x_1} \\ M_{y_1} \\ Z_1 \\ M_{x_2} \\ M_{y_2} \\ Z_2 \end{Bmatrix} = \left[\begin{array}{ccc:ccc} 0 & -t & 0 & & & \\ t & 0 & 0 & & & \\ 0 & 0 & 2 & & & \\ \hdashline & & & 0 & -t & 0 \\ & & & t & 0 & 0 \\ & & & 0 & 0 & 2 \end{array} \right] (\hat{\mathbf{K}}_w)_{1\text{-}2} \left[\begin{array}{ccc:ccc} 0 & t/2 & 0 & & & \\ -t/2 & 0 & 0 & & & \\ 0 & 0 & 1 & & & \\ \hdashline & & & 0 & t/2 & 0 \\ & & & -t/2 & 0 & 0 \\ & & & 0 & 0 & 1 \end{array} \right] \begin{Bmatrix} \theta_{x_1} \\ \theta_{y_1} \\ w_1 \\ \theta_{x_2} \\ \theta_{y_2} \\ w_2 \end{Bmatrix} \quad (15\text{d})
$$

$$
= (\mathbf{K}_w)_{1\text{-}2} \begin{Bmatrix} \theta_{x_1} \\ \theta_{y_1} \\ w_1 \\ \theta_{x_2} \\ \theta_{y_2} \\ w_2 \end{Bmatrix} \quad (15\text{e})
$$

Carrying out the triple matrix product of Eq. (15d) gives the shear web stiffness as

$$
(\mathbf{K}_w)_{1\text{-}2} = \frac{G}{4}\left(\frac{A_w}{L}\right)_{1\text{-}2} \begin{array}{cccccc} \theta_{x_1} & \theta_{y_1} & w_1 & \theta_{x_2} & \theta_{y_2} & w_2 \\ \end{array} \left[\begin{array}{ccc:ccc} y_{21}^2 & & & \multicolumn{3}{c}{\text{(SYMMETRIC)}} \\ -x_{21}y_{21} & x_{21}^2 & & & & \\ 2y_{21} & -2x_{21} & 4 & & & \\ \hdashline y_{21}^2 & -x_{21}y_{21} & 2y_{21} & y_{21}^2 & & \\ -x_{21}y_{21} & x_{21}^2 & -2x_{21} & -x_{21}y_{21} & x_{21}^2 & \\ -2y_{21} & 2x_{21} & -4 & -2y_{21} & 2x_{21} & 4 \end{array} \right] \quad (15\text{f})
$$

The other shear web stiffnesses are simply obtained by replacing 1-2 in Eq. (15f) with $i - j$ and then letting $i - j$ successively become 1-2, 2-3, and 3-1. The results then apply to the triangle arbitrarily oriented in the xy-plane.

E. Overall Element Stiffness Matrix

The total stiffness matrix is now the sum of the contributions from the cover sheets and three shear webs. These are given by Eqs. (12c) and (15f), where the latter is written out in full for each of the shear webs. The resulting stiffness equation is of the form

$$
\begin{Bmatrix} M_{x_1} \\ M_{y_1} \\ Z_1 \\ M_{x_2} \\ M_{y_2} \\ Z_2 \\ M_{x_3} \\ M_{y_3} \\ Z_3 \end{Bmatrix} = (\mathbf{K}_b + (\mathbf{K}_w)_{1\text{-}2} + (\mathbf{K}_w)_{2\text{-}3} + (\mathbf{K}_w)_{3\text{-}1}) \begin{Bmatrix} \theta_{x_1} \\ \theta_{y_1} \\ w_1 \\ \theta_{x_2} \\ \theta_{y_2} \\ w_2 \\ \theta_{x_3} \\ \theta_{y_3} \\ w_3 \end{Bmatrix} \quad (16)
$$

The total stiffness matrix of Eq. (16) applies to the arbitrarily oriented triangle as shown in Fig. 8.
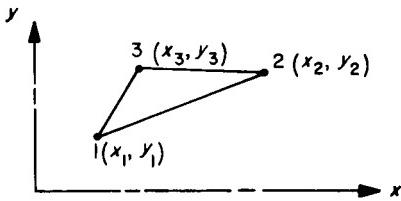
Fig. 8. Triangular sandwich element with arbitrary orientation in the xy-plane

F. Stresses

1. Cover sheets. The stiffness method solution provides the nodal displacements for each element. In terms of these displacements it is a simple calculation to find the internal stresses.

For the sandwich element, the stiffness solution will yield θ_{x_1}, θ_{y_1}, and w at each node. The corresponding u and v displacements can then be calculated from Eq. (3a). For any element, the cover sheet stresses are then given by

$$\left\{ \begin{array}{c} \sigma_x \\ \sigma_y \\ \tau_{xy} \end{array} \right\} = [S] \left\{ \begin{array}{c} u_a \\ v_a \\ u_b \\ v_b \\ u_c \\ v_c \end{array} \right\} \qquad (17a)$$

Stress matrix S is given as Eq. (18a), Ref. 5. In the reference, the triangle is oriented as shown in Fig. 2b. Rewriting S, as given in Ref. 5, to apply to the case in which the triangle is oriented as in Fig. 8 gives

$$S = \frac{E}{2(1 - \nu^2)\,A} \begin{bmatrix} y_{23} & \nu x_{32} & y_{31} & \nu x_{13} & y_{12} & \nu x_{21} \\ \nu y_{23} & x_{32} & \nu y_{31} & x_{13} & \nu y_{12} & x_{21} \\ \lambda_1 x_{32} & \lambda_1 y_{23} & \lambda_1 x_{13} & \lambda_1 y_{31} & \lambda_1 x_{21} & \lambda_1 y_{12} \end{bmatrix}$$

$$(17b)$$

Stresses in the bottom cover are equal to those in the top cover but are of opposite signs.

In many instances, the stiffness solution will be carried out in some reference system of coordinates which is convenient for the overall problem. Therefore, this should be taken into account prior to using Eq. (17a). In Eq. (17a), it is assumed that the displacements $u_{a_1} \cdots$,

etc., are given in terms of local coordinates for the specific element. Figure 2b shows the local coordinate axes system for an individual triangular element.

Stresses obtained from Eq. (17a) are the bending stresses for the actual solid structure. As such, they are directly related to the moments per inch (m_x, m_y, and m_{xy}) of plate theory. The equation can be shown as

$$\left\{ \begin{array}{c} m_x \\ m_y \\ m_{xy} \end{array} \right\} = \frac{t^2}{6} \left\{ \begin{array}{c} \sigma_x \\ \sigma_y \\ \tau_{xy} \end{array} \right\} \qquad (17c)$$

It should be noted that the stress σ_x in Eq. (17c) corresponds to m_x, etc. This is the convention of plate theory. It is not in agreement with the notation of this report as established in Fig. 4a and Eq. (6a).

2. Shear webs. The problem is to calculate the shear stresses in the actual solid plate. Again, these must be found from the solution obtained by using the sandwich element.

Since the nodal displacements are known, the corresponding nodal forces can be found from the element stiffness equation. It is convenient to think of these forces as follows: if applied to the single element they will produce the same nodal deflections experienced by the element when it deforms as one unit of the entire finite element assemblage under the applied loads or other disturbances. In particular, the Z_i nodal forces are of interest when shear stresses are to be calculated. Figure 9 shows these Z forces and the statically equivalent shear flows (q_{i-j}, lb/in.) on sections of the solid plate cut along the three edges of the triangle. The shear flow is equal to the shear stress times the plate thickness or

$$\tau_{i-j} = \frac{q_{i-j}}{t} \qquad (18a)$$

Initially, it is more convenient to use q than τ.
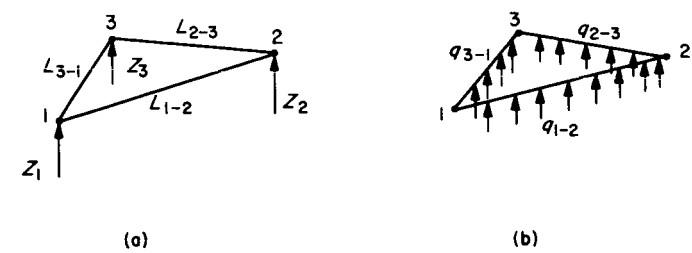
Fig. 9. Nodal shear forces on sandwich element (a) and shear flows on actual solid element (b)

Shear flows in Fig. 9b are related to the nodal forces of Fig. 9a by putting

$$Z_1 = [q_{1-2} L_{1-2} + q_{3-1} L_{3-1}]/2$$

$$Z_2 = [q_{1-2} L_{1-2} + q_{2-3} L_{2-3}]/2$$

$$Z_3 = [q_{2-3} L_{2-3} + q_{3-1} L_{3-1}]/2$$

Solving for the shear flows

$$\begin{Bmatrix} q_{1-2} L_{1-2} \\ q_{2-3} L_{2-3} \\ q_{3-1} L_{3-1} \end{Bmatrix} = \begin{bmatrix} 1 & 1 & -1 \\ -1 & 1 & 1 \\ 1 & -1 & 1 \end{bmatrix} \begin{Bmatrix} Z_1 \\ Z_2 \\ Z_3 \end{Bmatrix} \quad (18b)$$

The shear forces of Fig. 9a must satisfy equilibrium. This is so because these forces have been calculated from the known displacements and stiffness equation for the element.

Consequently

$$Z_1 + Z_2 + Z_3 = 0 \quad (18c)$$

Substituting Eq. (18c) into Eq. (18b) yields

$$q_{1-2} = - 2Z_3/L_{1-2}$$

$$q_{2-3} = - 2Z_1/L_{2-3} \quad (18d)$$

$$q_{3-1} = - 2Z_2/L_{3-1}$$

From these shear flows, it is now possible to calculate the shear stresses in the element.

First, consider a section of the solid plate cut normal to the x-axis. For convenience, take the perpendicular from node 3 to edge 1-2 (Fig. 10a). Let the shear flow

on a section at this line be q_x. Then, considering forces on the portion of the triangle to the left of the cut and imposing equilibrium

$$q_{1-2} x_3 + q_{3-1} L_{3-1} + q_x y_3 = 0$$

Solving for q_x and using Eq. (18d)

$$q_x = 2(Z_2 + Z_3 x_3/L_{1-2})/y_3 \quad (18e)$$

The corresponding transverse shear stress is

$$\tau_{xz} = q_x/t \quad (18f)$$

This shear stress is constant for the element.

Next, consider a section cut parallel to the x-axis. It is convenient to select this section at the edge 1-2 as shown in Fig. 10b. Then, again imposing equilibrium, and letting the shear flow on the section be q_y, it is found that

$$q_y = - q_{1-2} \quad (18g)$$

and the shear stress by

$$\tau_{yz} = q_y/t = 2Z_3/L_{1-2} t \quad (18h)$$

This stress is also constant on any section cut parallel to the x-axis.

3. Alternative procedures. The above stress calculations are simple because they follow directly from the stiffness method solution. Improved accuracy may be achieved by using various refinements on the basic procedures. Reference 11 describes some of these refinements.

III. Examples—Thin Plates and Shells

A. Flat Plates

Figure 11a illustrates a flat plate of aspect ratio 2. Edges may be either simply supported or clamped. Loading will be either uniformly distributed over the plate area, or concentrated at the midpoint. Figure 11b shows the elements corresponding to the case $n = 2$. Because of symmetry, only one quadrant of the plate needs to be considered in the analysis. For the case $n = 4$, each subrectangle of Fig. 11b is divided into four equal rectangles, which, in turn, are divided into two triangles,


Fig. 10. Sections in solid element used in determining transverse shear stresses
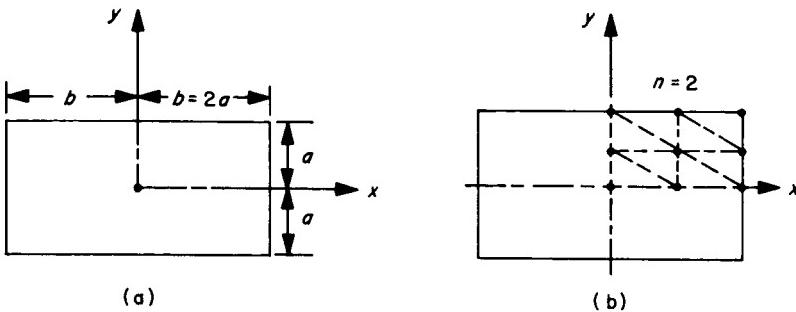
Fig. 11. Rectangular plate represented by triangular elements

as in the case shown in the figure. A similar definition is used for other values of n. In all, solutions were obtained for $n = 1, 2, 4$, and 8.

The displacement at the midpoint may be written as

$$w_{max} = \alpha_c \frac{Pa^2}{D} \quad \text{(concentrated load)} \quad (19a)$$

$$w_{max} = \alpha_d \frac{qa^4}{D} \quad \text{(distributed loading)} \quad (19b)$$

where

$$D = Et^3/12(1-\nu^2)$$

as in plate theory.

Reference 12 gives the exact solution based on plate theory. Table 1 gives the stiffness solutions for the maximum deflection. These solutions agree remarkably well with the exact solution, even when the idealization of elements is quite coarse.

Bending stresses in the plate are also of interest. Only the case of the simply supported plate under a uniformly distributed loading will be presented herein. Following

Table 1. Maximum deflection—rectangular plate problems

n	Simply supported		Clamped	
	α_c	α_d	α_c	α_d
1	0.0219	0.0109	0.0119	0.0059
2	0.0191	0.0108	0.0098	0.0039
4	0.0174	0.0103	0.0082	0.0029
8	0.0168	0.0102	0.0075	0.0026
Exact solution	0.0165	0.0101	0.0072	0.0025

the convention of Ref. 12, the internal moment (in.-lb/in.) acting along the y-axis (Fig. 11a) will be compared against the exact result. In Ref. 12, this moment is represented by $(M_x)_{x=0}$, while in the notation of this report (Fig. 4a) it is termed $(M_y)_{x=0}$. Reference 12 gives values for β where

$$(M_x)_{x=0} = \beta q a^2$$

and

q is the distributed loading in psi.

Figure 12 shows β as taken from Ref. 12. In addition, the stiffness solutions, for the idealizations $n = 4$ and $n = 8$, are also shown. To obtain the stiffness solution on the y-axis, values for M_x were averaged for each pair of triangles within a given subrectangle. This average value was then taken to hold at the centroid of the subrectangle. Plotting these results and extrapolating the curves to the y-axis then gave the desired results for M_x.
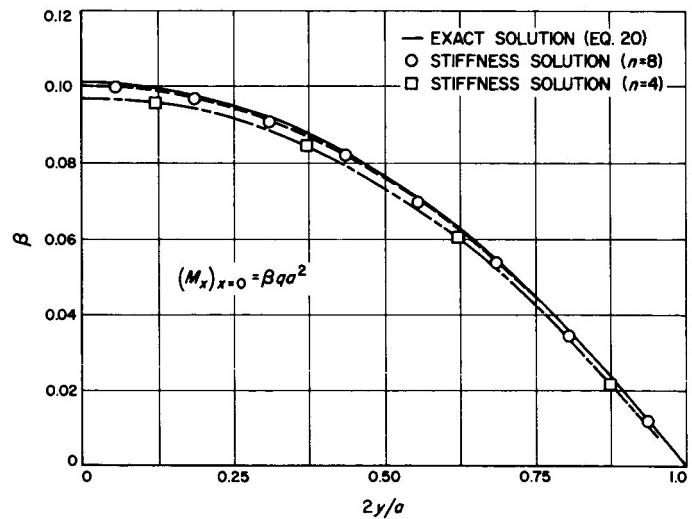

Fig. 12. Bending moment (M_x) along y-axis for the uniformly loaded, simply supported rectangular plate

B. Spherical Cap

A simple shell is represented by the spherical cap under uniform normal pressure. The theoretical solution may be found in Ref. 12, pp. 553–554. Figure 13 illustrates the problem.
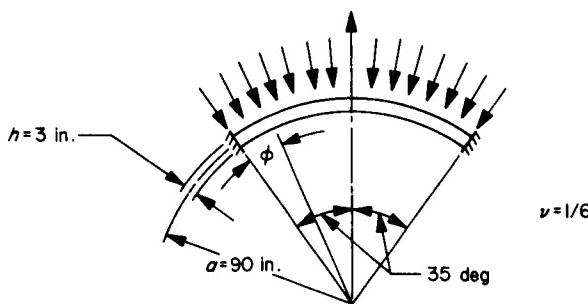

Fig. 13. Section of spherical cap under uniform normal pressure

The idealizations represented by $n = 3$ and $n = 4$ are shown in Figs. 14a and 14b, respectively. Other values of n are similarly defined. It should be noted that a complete quadrant of the cap was used in the stiffness analysis. This is basically unnecessary because of the symmetry in this problem; however, the program in use at the time the solution was obtained was such that it was convenient to use the full quadrant.

For this problem, the finite element substitution was made as illustrated by Fig. 14c. The curved arcs were replaced by chords. An interior node was then established by the intersection of straight lines joining opposite sides of the quadrilateral. Using this interior node, each quadrilateral was then represented by four triangles. These four triangles were then forced to lie in a single plane. This procedure was followed for the subareas shown in Figs. 14a and 14b.

Details of the stiffness method solution in treating this problem will not be given here. Within any quadrilateral, stresses were averaged for the four triangles and then said to apply at the interior node.

Deflections normal and tangential to the shell are shown in Fig. 15. The tangential deflections point radially outward from the origin in a plan view. This figure shows that if $n = 5$, the stiffness solution duplicates the deflections obtained by exact theory.
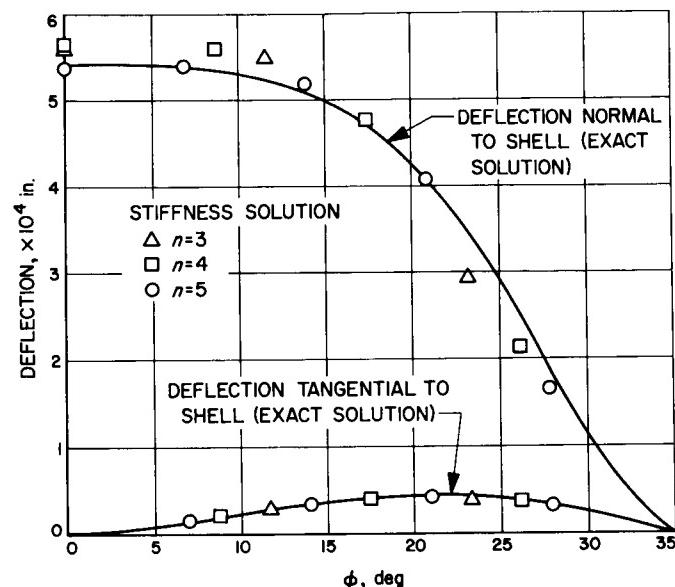
Fig. 15. Deflections for spherical cap

The meridional moments, $M\phi$, which again are proportional to the corresponding internal stresses, are shown in Fig. 16. Again, good agreement exists between exact and finite element solutions.

Fig. 14. Idealization of spherical cap into finite triangular elements
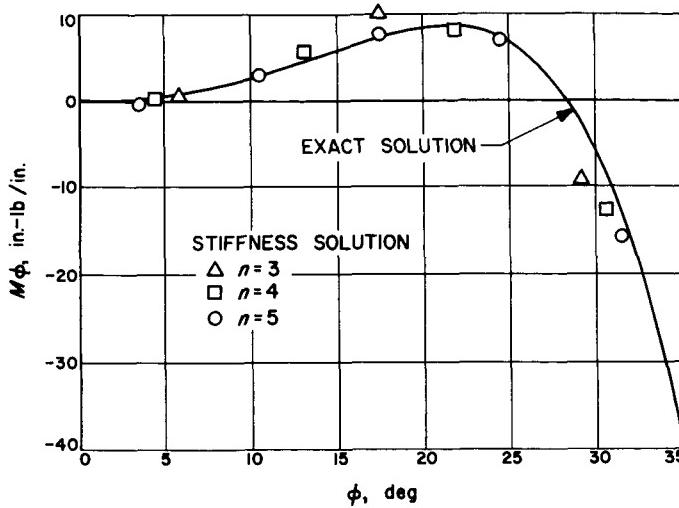
Fig. 16. Meridional bending moment, spherical cap

Finally, the so-called hoop stresses, N_θ, are shown in Fig. 17. The idealization represented by $n = 5$ was necessary to obtain satisfactory agreement with correct results in this case.
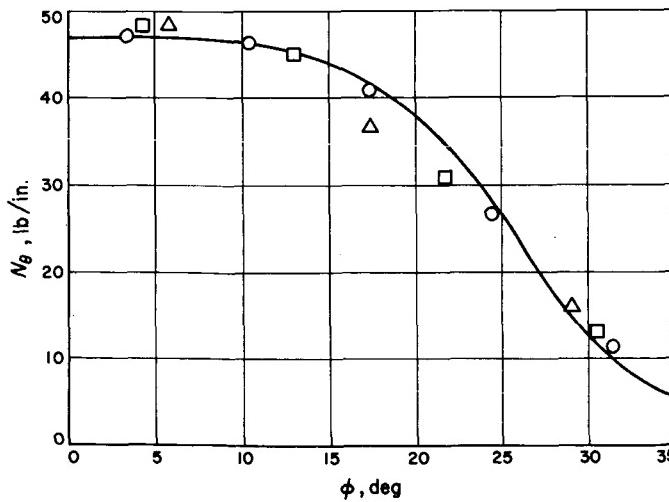
Fig. 17. Hoop stress due to bending, spherical cap

C. Remarks

The above results illustrate the remarkable ability of the flat sandwich element to predict the behavior of thin plates and shells. Also, from the structural analyst's point-of-view, it is important to recognize that comparatively few elements are needed to achieve results of sufficient accuracy to successfully carry out a structural design.

IV. Orthotropic Panels

A. Nature of Problem

Plate and shell structures having orthotropic properties are frequently used by the structural designer. A variety of design possibilities exist, bringing some confusion into the subject. Several basic types of structures will be studied herein to show how they may be represented by the triangular sandwich element. The discussion will be confined to rectangular panels whose sides are parallel to the principal directions of orthotropy.

At the outset, the prime question which arises is the following: can the sandwich element discussed in this report represent the orthotropic panel to an acceptable degree of accuracy? To do so, it must have different bending stiffness in two mutually perpendicular directions. Before considering this question further, the orthotropic panels which are to be investigated will be briefly defined.

B. Panels Having Material Orthotropy

1. Solid plate. This case differs from the conventional thin plate because the material properties are orthotropic, rather than isotropic. Plywood, in which the grain of alternate plys runs at right angles to each other, represents a generalization of the basic case.

2. Sandwich panels. These consist of identical upper and lower cover plates separated by a shear core. The sandwich triangle will directly represent this case when the cover sheets and shear core are isotropic. It is also of interest to consider the more general case; i.e., when the panel covers are orthotropic.

C. Panels Having Geometric Orthotropy

Examples of this type of panel have been suggested, tested, and used. Of long standing is the panel made up of corrugated sheet held between identical top and bottom covers. Or, alternatively, the interior structure may consist of equally spaced stiffeners such as I–sections, channels, or even tubes. Panels of this type are orthotropic in nature, although the material may be isotropic throughout. A generalization occurs when the cover sheets are orthotropic.

D. Orthotropic Stress–Strain Law

Assume a rectangular sheet for which the two principal directions of material properties are parallel to the

x and y edges, respectively. The stress-strain relation for such a sheet may then be expressed (Ref. 13) as

$$\begin{Bmatrix} \sigma_x \\ \sigma_y \\ \tau_{xy} \end{Bmatrix} = \frac{1}{1 - \nu_1 \nu_2} \begin{bmatrix} E_1 & \nu_2 E_1 & 0 \\ \nu_1 E_2 & E_2 & 0 \\ 0 & 0 & 2G \end{bmatrix} \begin{Bmatrix} \epsilon_x \\ \epsilon_y \\ \gamma_{xy}/2 \end{Bmatrix}$$

(20a)

Symmetry requires that

$$\nu_2 E_1 = \nu_1 E_2 \qquad (20b)$$

Equations (20a) and (20b) indicate that four material constants are required to define the orthotropic, two-dimensional case. However, as for the isotropic material, no coupling exists between normal and shearing terms.

As noted in Ref. 13, the above material properties are often usefully replaced by defining

$$E = E_1, \quad kE = E_2, \quad \nu = \nu_1, \quad k\nu = \nu_2$$

$$G = \lambda E / 1 - k\nu^2 \qquad (21)$$

The four independent constants are then E, ν, k, and λ. In terms of these constants, Eq. (20a) becomes

$$\begin{Bmatrix} \sigma_x \\ \sigma_y \\ \tau_{xy} \end{Bmatrix} = \frac{E}{1 - k\nu^2} \begin{bmatrix} 1 & k\nu & 0 \\ k\nu & k & 0 \\ 0 & 0 & 2\lambda \end{bmatrix} \begin{Bmatrix} \epsilon_x \\ \epsilon_y \\ \gamma_{xy}/2 \end{Bmatrix}$$

(22)

Hence, either Eq. (20a) or Eq. (22) may be used to represent the two-dimensional orthotropic sheet.

E. Modeling an Orthotropic Panel With a Sandwich Element

The orthotropic plate will be taken as shown in Fig. 18. A typical choice of triangular elements is also shown. This idealization agrees with that used in analyzing flat plates in bending (Fig. 11b).

An obvious basis for providing the triangular sandwich element with orthotropic bending properties is to use orthotropic cover sheets. By assigning the proper values to E_1, E_2, G, and ν_1 (or ν_2) the stiffness can be altered at will in the two perpendicular directions. It would then appear that the sandwich element could become capable of representing the orthotropic panel.
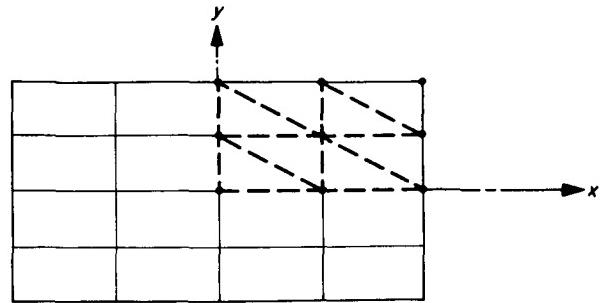
Fig. 18. Orthotropic plate and idealization into finite element triangles

Section II-B-2 provided the basis for modeling the conventional thin plate with the sandwich element. The basic requirement was that the bending stiffness be the same for actual plate and sandwich model. A similar requirement will now be imposed in modeling the orthotropic panels by the sandwich element.

F. Modeling the Solid Orthotropic Plate

1. Solid single-ply section.

a. Cover sheets. In the x-principal direction put

$$E_{x_s} I_{x_s} = E_{x_p} I_{x_p}$$

where subscript s stands for the sandwich element and p for the true structural panel. As for the isotropic sandwich element (Fig. 5), the moment of inertia I_{x_s} is given by

$$I_{x_s} = hd^2/2$$

And, if t is the thickness of the actual panel

$$I_{x_p} = t^3/12$$

By putting

$$E_{x_s} = E_{x_p} \quad \text{and} \quad d = t$$

it is again seen that

$$h = t/6$$

where h is the thickness of the orthotropic cover sheet on the sandwich element. A similar result is obtained in the y-principal direction by choosing

$$E_{y_s} = E_{y_p}$$

Consequently, the orthotropic cover sheets on the sandwich element permit the bending stiffness in the principal directions to match those of the actual orthotropic plate.

b. Shear webs. The shear web thicknesses can be determined by using Eq. (15f) with shearing modulus G equal to the value known for the actual plate.

2. Solid multi-ply section.

a. Cover sheets. Next, a multi-ply section, similar to plywood is considered. The plate consists of lamina, similar to that illustrated in Fig. 19, with a 90-deg change in principal directions from one ply to the next. Symmetry about a horizontal midplane is assumed. Figure 19 represents a unit strip of such a panel section. Any number of laminae may be used as long as the symmetry condition is maintained. For the actual panel section of n lamina, let

$$\sum_{i=1}^{n} (E_x I_x)_i = (E_{x_p})_{av}\, t^3/12$$

where the summation is over the lamina making up the panel. This expression can be used to determine $(E_{x_p})_{av}$.

Now equate

$$E_{x_s} I_{x_s} = (E_{x_p})_{av}\, t^3/12$$

where

$$I_{x_s} = hd^2/2$$

Then, by letting

$$d = t \quad \text{and} \quad E_{x_s} = (E_{x_p})_{av}$$

it is again found that $h = t/6$.
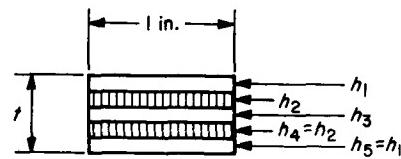
Fig. 19. Multi-ply orthotropic plate section

A similar result is obtained by considering terms in the y-direction. It is then necessary to use

$$E_{y_s} = (E_{y_p})_{av}$$

b. Shear webs. The value of G to be used in Eq. (15f) is known from the material properties of the orthotropic lamina. If the individual laminae have different values of G, a weighted average can be used in determining the shear web areas of the sandwich element.

3. Sandwich panel.
No difficulty is encountered with this type of panel. The sandwich element cover skins can directly duplicate the orthotropic covers of the actual panel. Also, G of the panel shear core can be used directly in Eq. (15f) to determine the sandwich element shear webs. The depth, d, of the sandwich element should exactly equal that of the actual structural panel.

4. Panels having geometric orthotropy.
Typical examples of panels having geometric orthotropy are illustrated in Fig. 20. Orthotropy exists even when the material is isotropic throughout.

a. Isotropic cover sheets. Considering the x-direction, first calculate $(I_{x_p})_{av}$. This is the average moment of inertia of both cover sheets and interior stiffeners per inch (measured along y-axis). Since $(I_{x_p})_{av}$ is known, calculate an equivalent solid plate thickness, t, by requiring

$$t^3/12 = (I_{x_p})_{av}$$
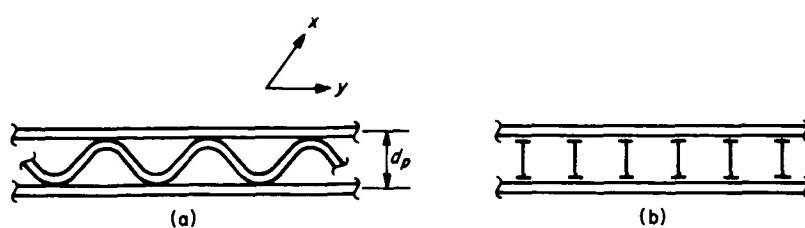
Fig. 20. Geometrically orthotropic panels

The problem can now be regarded in the same manner as the previous solid plate (Subsection F-1). In this way, the triangular sandwich element should be modeled on the basis of

$$h = t/6$$

and

$$E_{x_s} = E_{x_p}$$

where h is again the element cover skin thickness. If E_x of actual plate covers and stiffeners are not equal, E_{x_p} must be replaced by a suitably determined $(E_{x_p})_{av}$.

A similar calculation can be made in the y-direction. Stiffeners are now ineffective in contributing to I_{y_p} (Fig. 20). For equal bending stiffness in the y-direction

$$E_{y_s} I_{y_s} = E_{y_p} I_{y_p}$$

For the sandwich triangle, I_{y_s} is the same as I_{x_s}; i.e., $ht^2/2$. Hence, the last equation can be used to find E_{y_s}. This completes the determination of the finite element cover sheets for this case.

b. *Orthotropic cover sheets.* First, calculate I_{x_p} (per inch) for plate covers and stiffening material. Then, find the equivalent solid plate thickness, t, from

$$t^3/12 = I_{x_p} \text{(covers)} + I_{x_p} \text{(stiffeners)}$$

Then, find $(E_{x_p})_{av}$ by requiring that

$$(E_{x_p})_{av} t^3/12 = E_{x_p} I_{x_p} \text{(covers)} + E_{x_p} I_{x_p} \text{(stiffeners)}$$

This last expression determines $(E_{x_p})_{av}$ for the panel. The sandwich triangle can now be introduced. For equal bending stiffnesses, between sandwich and actual panel in the x-direction

$$(E_x)_s hd^2/2 = (E_{x_p})_{av} t^3/12$$

Letting

$$d = t$$

$$E_{x_s} = (E_{x_p})_{av}$$

it is found that

$$h = t/6$$

In the y-direction, the stiffeners are once again ineffective in providing bending stiffness. Hence, I_{y_p} is due

entirely to the cover sheets. If E_{y_p} is used as the appropriate panel cover sheet modulus, and t and h are retained as determined above, equal bending stiffnesses in the y-direction will result if

$$E_{y_s} ht^2/2 = E_{y_p} I_{y_p}$$

This last equation then determines E_{y_s} for the triangle.

c. *Shear webs.* As may be implied from Fig. 20, geometrically orthotropic panels will have small shear flexibility in comparison to bending. Or, in other terms, the strain energy in the triangular element shear webs will be small compared to that in the cover sheets. As a result, the overall stiffness solution will not be sensitive to appreciable errors in determining the shear web thicknesses. The shear webs are necessary but their areas are not a sensitive factor insofar as final results are concerned. This is further discussed in Section VI-C.

With this in mind the shear web areas can be determined by using the equivalent solid plate thickness, t, as calculated above, plus G for the actual panel material. If covers and stiffeners are of different materials, a reasonably calculated average G should be used in Eq. (15f).

V. Stiffness Matrix Derivation—Orthotropic Cover Sheet

The discussion in Section IV indicates that a sandwich finite element can be used to represent several types of orthotropic panels if the element is provided with orthotropic cover sheets. The key to this development lies in finding the stiffness matrix for the orthotropic, two-dimensional sheet. Once this stiffness matrix is known, it may be used in place of the corresponding isotropic relation, Eq. (11c), in deriving the total element stiffness matrix. Fortunately, the derivation of the stiffness matrix for the orthotropic sheet is no more difficult than for the more usual isotropic case.

Orthotropy is defined by either Eq. (20a) or Eq. (22). Axes x and y agree in direction with the principal material directions. Transformation of the above equations to arbitrary x', y' axes is not difficult; however, such generality is not necessary when idealizing panels in the manner illustrated in Fig. 18. As a result, the derivation will be carried out for the case shown in Fig. 21.

Consider either Eq. (20a) or Eq. (22) to be expressed as

$$\sigma = \xi \, \varepsilon \qquad (23)$$
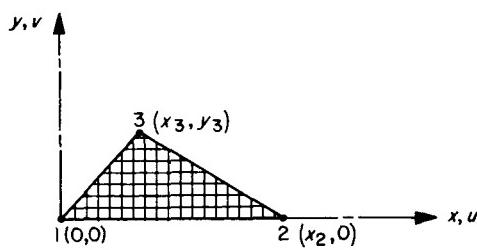
Fig. 21. Orthotropic triangular cover sheet

Writing $u(x, y)$ and $v(x, y)$ at each node of the triangle, and solving the resulting set of six equations for a, b, $\cdots$, f yields

$$a = u_1$$

$$b = \frac{u_2 - u_1}{x_2}$$

$$c = \frac{x_3 - x_2}{x_2 y_3} u_1 - \frac{x_3}{x_2 y_3} u_2 + \frac{1}{y_3} u_3$$

$$d = v_1$$

$$e = \frac{v_2 - v_1}{x_2}$$

$$f = \frac{x_3 - x_2}{x_2 y_3} v_1 - \frac{x_3}{x_2 y_3} v_2 + \frac{1}{y_3} v_3$$

Either equation may be used and the choice made will specify ξ. The strain energy U in the sheet is then given by

$$U = \frac{1}{2} \iiint \varepsilon^T \sigma \, dx \, dy \, dz = \frac{h}{2} \iint \varepsilon^T \sigma \, dx \, dy$$

Substituting Eq. (23)

$$U = \frac{h}{2} \iint \varepsilon^T \xi \, \varepsilon \, dx \, dy \tag{24}$$

It is known that the correct choice of displacement functions for this case is

$$u(x, y) = a + bx + cy$$

$$v(x, y) = d + ex + fy$$

Then, since

$$\epsilon_x = \frac{\partial u}{\partial x} = b$$

$$\epsilon_y = \frac{\partial v}{\partial y} = f$$

$$\gamma_{xy} = \frac{\partial u}{\partial y} + \frac{\partial v}{\partial x}$$

$$= c + e$$

it follows that

$$
\begin{Bmatrix} \epsilon_x \\ \epsilon_y \\ \gamma_{xy}/2 \end{Bmatrix}
=
\begin{bmatrix}
-\dfrac{1}{x_2} & 0 & \dfrac{1}{x_2} & 0 & 0 & 0 \\[2mm]
0 & \dfrac{x_3 - x_2}{x_2 y_3} & 0 & -\dfrac{x_3}{x_2 y_3} & 0 & \dfrac{1}{y_3} \\[2mm]
\dfrac{x_3 - x_2}{2x_2 y_3} & -\dfrac{1}{2x_2} & -\dfrac{x_3}{2x_2 y_3} & \dfrac{1}{2x_2} & \dfrac{1}{2y_3} & 0
\end{bmatrix}
\begin{Bmatrix} u_1 \\ v_1 \\ u_2 \\ v_2 \\ u_3 \\ v_3 \end{Bmatrix}
\tag{25a}
$$

or

$$\varepsilon = \Theta \, \mathbf{u} \tag{25b}$$

Equation (25b) can now be substituted into Eq. (24). Since the integrand is independent of x and y, the result may be written as

$$U = \frac{1}{2} \mathbf{u}^T \left(h \, A \, \Theta^T \xi \, \Theta \right) \mathbf{u} \tag{26}$$

where A is the area of the triangle. The form of Eq. (26) then provides the following for the orthotropic sheet stiffness matrix:

$$\mathbf{K} = hA \, \Theta^T \xi \, \Theta \tag{27}$$

Since Θ and ξ are known, it is now simple to complete the calculation for the stiffness matrix of the orthotropic sheet.

VI. Effect of Triangle Geometry on Element Stiffness Matrix

A. Definition of Terms

Let θ_i be the angle between the two edges of the triangle which meet at node i. Then the geometric cases of interest are defined by $\theta_i < 90$ deg, $\theta_i = 90$ deg and $\theta_i > 90$ deg. In this connection, assume θ_i to be the largest angle included between two edges of the triangle.

Stiffness matrix **K** for the triangular element will be symmetric. Consequently, its eigenvalues will always be real. Depending on how the stiffness matrix is obtained, these values may, however, be all positive, or one or more may be zero, or even negative. This last possibility signals a defect in the element stiffness matrix.

By matrix transformation, it is possible to replace **K** with an equivalent diagonal matrix. If this is done, the following definitions apply if all elements on the diagonalized form of **K** are:

(1) Positive, **K** is said to be positive definite.

(2) Positive, with one or more being zero, **K** is said to be positive semi-definite.

(3) Positive, but with one or more being negative, **K** is said to be indefinite.

A stiffness matrix which is indefinite is unacceptable. The negative element in the diagonalized form indicates that, for some applied force, the corresponding displacement will oppose the direction of the load. This is not characteristic of physical systems. Consequently, an element stiffness matrix should always be positive definite, or at least positive semi-definite.

B. Triangle Geometry and Character of Stiffness Matrix

In a numerical study, Utku and Melosh showed that the triangular sandwich element had the following property:

1. positive definite if $\theta_i < 90$ deg

2. positive semi-definite if $\theta_i = 90$ deg

3. indefinite if $\theta_i > 90$ deg

These results are discussed in Ref. 14. The overall effects of this behavior are not known at present. Apparently, when $\theta_i > 90$ deg, the diagonalized form of **K** contains one negative element; if $\theta_i = 90$ deg, one zero term occurs. An idealization containing triangles having $\theta_i > 90$ deg can be somewhat artificially treated so as to avoid numer-ical difficulties or poor results. It can be stated that, having recognized the shortcoming, steps should be taken to avoid it by somehow circumventing the development of an indefinite form for the element **K** matrix. Utku and Melosh suggest several ways of doing this (Ref. 14). The scheme used in the COSMOS and SAMIS computer programs is to use absolute values on certain minor terms which are responsible for the generation of an indefinite stiffness matrix. Although indefensible on theoretical grounds, experience shows that this artifice works. For example, the idealization shown in Fig. 14 contains two triangles, in each quadrilateral, for which $\theta_i > 90$ deg. Yet, by using the scheme previously mentioned, excellent data have been obtained. As shown in Section III-B, extensive experience with the triangular sandwich element supports this conclusion.

The reason for the generation of the indefinite **K** matrix will be discussed in this section of the report. For certain classes of triangles, having $\theta_i > 90$ deg, an alternative suggestion will be made to avoid the indefinite stiffness matrix. The suggestion will be based on a logical specialization of the theory which has been used in deriving the element **K** matrix.

A useful idealization for rectangular planforms is illustrated in Fig. 22. Each such subrectangle is divided into four triangles. This automatically introduces two triangles for which $\theta_i > 90$ deg.

The idealization illustrated in Fig. 22 is essentially the same as that used in analyzing the spherical cap of Fig. 14. Whether the triangles are plane stress elements used for analyzing a two-dimensional continuum, or sandwich elements for representing plate or shell bending, stresses are always obtained with superior accuracy if the idealization shown in Fig. 22 is adopted. The stress at the centroid of each subrectangle is taken as the average of the stress values for each of the component triangles. Because of this, triangles of the type shown in Fig. 22, and with $\theta_i > 90$ deg, become of particular importance. They will be given special attention in this report.
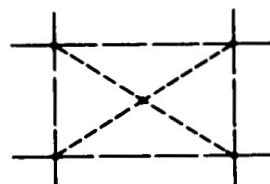

**Fig. 22. Idealization of rectangular forms into four triangles**
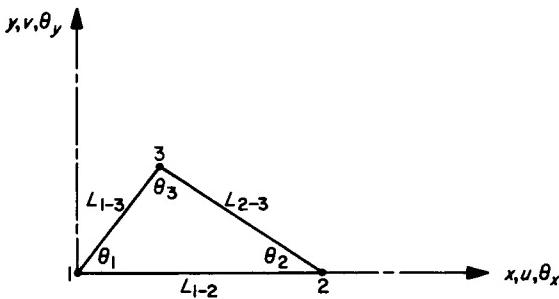
Fig. 23. Triangle with $\theta_3 > 90$ deg

C. Indefinite Form of Triangular Element Stiffness Matrix

As previously mentioned, Utku and Melosh discovered by numerical calculations that $\mathbf{K}$ for the sandwich element becomes indefinite when $\theta_i > 90$ deg. To examine this on the basis of the derivation given in this report, the single element $k_{\theta_{y_1} \theta_{y_1}}$ will be written for a triangle taken as shown in Fig. 23.

From Eqs. (12c) and (15f), where the latter must be written for all shear webs, it can be shown that

$$k_{\theta_{y_1} \theta_{y_1}} = \frac{Et^3 \phi}{24} (\lambda_1 x_{23}^2 + y_{23}^2) + \frac{G}{4}\left[\left(\frac{A_w}{L}\right)_{1-2} x_{21}^2 + \left(\frac{A_w}{L}\right)_{1-3} x_{31}^2 \right]$$

where

$\phi = \frac{1}{2}(1-\nu^2) A$

$\lambda_1 = (1-\nu)/2$

$A_w = $ shear web area

$x_{ij} = x_i - x_j$.

The shear web areas are obtained from Eq. (10) as

$$\left(\frac{A_w}{L}\right)_{1-2} = \frac{t}{8A}(-L_{1-2}^2 + L_{2-3}^2 + L_{3-1}^2)$$

$$\left(\frac{A_w}{L}\right)_{1-3} = \frac{t}{8A}(L_{1-2}^2 + L_{2-3}^2 - L_{1-3}^2)$$

Applying the Law of Cosines to the triangle in Fig. 23

$$L_{1-2}^2 = L_{1-3}^2 + L_{2-3}^2 - 2L_{1-3} L_{2-3} \cos \theta_3$$

$$L_{1-3}^2 = L_{1-2}^2 + L_{2-3}^2 - 2L_{1-2} L_{2-3} \cos \theta_2$$

Substituting into the expression for $k_{\theta_{y_1} \theta_{y_1}}$ yields

$$k_{\theta_{y_1} \theta_{y_1}} = \frac{Et}{16(1+\nu)A}\left[\frac{t^2}{3(1-\nu)}\left(y_3^2 + \frac{1-\nu}{2} x_{23}^2 \right) \right.$$
$$\left. + \frac{L_{2-3}}{2}\{(L_{1-3}\cos\theta_3) x_{21}^2 + (L_{1-2}\cos\theta_2) x_{31}^2 \} \right]$$

Now, a special case is taken in which $\theta_1 = \theta_2 = 30$ deg (Fig. 23). Substituting this geometry then leads to

$$k_{\theta_{y_1} \theta_{y_1}} = \frac{Et}{64(1+\nu)A} L_{1-3}^2 \left(t^2 - \frac{3}{4} L_{1-3}^2 \right)$$

Since t is the thickness of the sandwich element, $k_{\theta_{y_1} \theta_{y_1}}$ will be negative. Hence, an applied moment M_{y_1} will cause a negative θ_{y_1} to occur. Due to symmetry, a similar condition will exist at node 2. This is physically unreasonable. It is this unexpected result which underlies the indefinite form of $\mathbf{K}$, as reported in Ref. 14.

It is now of interest to check the limiting case; i.e., the triangle for which $\theta_1 = \theta_2 = 45$ deg, $\theta_3 = 90$ deg. If this is done

$$k_{\theta_{y_1} \theta_{y_1}} = \frac{Et}{16(1+\nu)A}$$
$$\times \frac{L_{1-3}^2}{2}\left[\frac{t^2}{3(1-\nu)}\left(1 + \frac{1-\nu}{\sqrt{2}} \right) + \frac{L_{1-3}^2}{\sqrt{2}} \right]$$

which is always greater than zero. For this same case

$$k_{w_1 w_1} = \frac{Gt}{4A} L_{2-3}^2$$

Hence, the indefinite form of $\mathbf{K}$ is clearly dependent on θ_3.

Further insight into the problem is obtained by examining the shear web areas as given by Eq. (10). From Eq. (10)

$$\left(\frac{A_w}{L}\right)_{1-2} = \frac{t}{8A}(-L_{1-2}^2 + L_{2-3}^2 + L_{3-1}^2)$$

$$\left(\frac{A_w}{L}\right)_{2-3} = \frac{t}{8A}(L_{1-2}^2 - L_{2-3}^2 + L_{3-1}^2)$$

$$\left(\frac{A_w}{L}\right)_{3-1} = \frac{t}{8A}(L_{1-2}^2 + L_{2-3}^2 - L_{3-1}^2)$$

Substituting from the previous expression for L_{1-2}^2

$$\left(\frac{A_w}{L}\right)_{1-2} = \frac{t}{8A}(2L_{1-3}L_{2-3}\cos\theta_3)$$

When $\theta_3 > 90$ deg, shear web area $(A_w)_{1-2}$ becomes negative. The other two shear web areas remain positive. This result is general in that it is always the shear web area on the edge which is opposite to the obtuse angle which becomes negative. If $\theta_3 = 90$ deg, $(A_w)_{1-2}$ becomes equal to zero. For $\theta_3 < 90$ deg, all shear web areas are positive. Even when $(A_w)_{1-2}$ becomes negative, the total strain energy in shear, Eq. (9), remains positive. For example, in Eq. (9)

$$(A_w/L)_{1-2} + (A_w/L)_{1-3}$$

or

$$(A_w/L)_{1-2} + (A_w/L)_{2-3}$$

will always be positive. This is verified by substituting the above expressions for $(A_w/L)_{i-j}$.

It is the negative shear web area which is responsible for the indefinite K matrix. The scheme previously mentioned avoids this difficulty by using absolute values for shear web areas. If this is done, K never becomes indefinite. However, the energy balance leading to Eq. (10) is then upset. This still leads to an acceptable stiffness matrix because this energy is only a small part of the total energy in the strained element. Consequently, it can be "tampered with" without seriously impairing the ability of the element stiffness matrix for representing bending behavior. However, if a sandwich-type panel having considerable shear flexibility is to be analyzed, it is not certain that the absolute value scheme for shear web areas would lead to satisfactory results.

There is no known basis for completely overcoming this difficulty. In Section D below, an approximate correction is offered. This correction takes the shear energy of Eq. (9) into account.

D. Suggested Basis for Avoiding the Indefinite Form of K

The numerical work of Utku and Melosh (Ref. 14) and the above discussion indicates that the indefinite form of K is caused by the negative shear web area. Consequently, a basis for avoiding negative shear web areas will be proposed. The discussion will be centered on isosceles triangles of the type illustrated in Figs. 22 and 23 with $\theta_1 = \theta_2$.

When $\theta_3 < 90$ deg, no problem exists; all shear web areas are positive. When $\theta_3 = 90$ deg, $(A_w)_{1-2}$ becomes equal to zero. Thereafter, as θ_3 increases beyond 90 deg, $(A_w)_{1-2}$ becomes negative. It is this latter case which is of interest.

Equations (8) and (9) represent the transverse shear energy in the solid and sandwich elements, respectively. Equating these energies leads to the shear web areas as given by Eq. (10). The negative area then follows as soon as $\theta_3 > 90$ deg. No general basis for avoiding this situation seems to exist.

Consider now the case for which $\theta_3 = 90$ deg. Shear web area $(A_w)_{1-2}$ is then zero. Rather than permit this to become negative as θ_3 increases beyond 90 deg, impose the restriction that

$$(A_w)_{1-2} = 0$$

when

$$\theta_3 > 90 \text{ deg} \tag{28a}$$

Further, impose the restriction that

$$(A_w)_{1-3} = (A_w)_{2-3} = A_w$$

when

$$\theta_3 > 90 \text{ deg} \tag{28b}$$

Finally, replace the general deformation modes $(w_1 \neq w_2 \neq w_3)$ in Eqs. (8) and (9) with the average condition that

$$w_1 = w_2 = w_3 = w \tag{28c}$$

Under these restrictive assumptions, the energy equality between Eqs. (8) and (9) leads to

$$A_w = \frac{t}{8A}\left(\frac{L_{1-2}^2 + L_{2-3}^2 + L_{1-3}^2}{L_{1-3} + L_{2-3}}\right)L_{1-3}\,L_{2-3} \qquad (29)$$

This expression can then be used for the isosceles triangle with $\theta_3 > 90$ deg.

In applying Eq. (29) to panels having considerable shear flexibility, it may be worthwhile to introduce a numerical factor α such that

$$A_w^* = \alpha\,A_w \qquad (30)$$

The parameter α can then be assigned a numerical value such that the shear web energy under the above restrictions represents the best possible average for a range of values of $\theta_3 > 90$ deg. For conventional thin plates and shells, this is believed unnecessary due to the relative unimportance of the shear web terms.

Numerical data have not yet been secured with Eq. (29).

VII. Large Deflection and Stability Analysis

As mentioned in Section I, the triangular sandwich element can be used in carrying out large deflection and stability calculations on plates. It may also be applicable in this same sense to shells, although actual calculations have not yet been carried out.

The reason for this useful characteristic of the sandwich element is that it remains a flat surface while representing bending behavior. As a result, it remains compatible with the initial stress stiffness matrix developed by the author for a triangular element (Ref. 9). The ability of these two stiffness matrices for the triangle (sandwich element matrix of this report and the initial stress matrix of Ref. 9) to correctly predict plate stability and large deflection behavior was shown in Ref. 15. This opens the door for a finite element solution for many types of plates, in which stability or large deflections, as defined by the von Kármán equations is of interest.

References

1. Sutherland, W. H., *Calculation of a Stiffness Matrix for Out-of-Plane Bending of a Triangular Plate Element*, Loads and Acoustics Research Memorandum No. 15, The Boeing Company, Seattle, Wash., May 1960.

2. Ortega, M. A., *Calculation of the Deflection at the Center of a Square Plate With Clamped Edges Using Various Stiffness Matrices*, Struc. Anal. Research Memorandum No. 14, The Boeing Company, Seattle, Wash., May 1960.

3. Lunder, C. A., *Derivation of a stiffness Matrix for a Right Triangular Plate in Bending and Subjected to Initial Stresses*, Master of Science Thesis, Department of Aeronautics and Astronautics, University of Washington, Seattle, Wash., 1961.

4. McMahon, L. L., *Development and Application of the Direct Stiffness Method for Out-of-Plane Bending Using a Triangular Plate Element*, Master of Science Thesis, Department of Aeronautics and Astronautics, University of Washington, Seattle, Wash., 1962.

5. Turner, M. J., Clough, R. W., Martin, H. C., and Topp, L. J., "Stiffness and Deflection Analysis of Complex Structures," *J. Aeronaut. Sci.*, Vol. 23, No. 9, pp. 805–823, Sept. 1956.

6. Melosh, R. J., "A Flat Triangular Shell Element Stiffness Matrix," *Proc. Conf. on Matrix Methods in Struc. Mechs.*, AFFDL-TR-66-80, pp. 503–514, U. S. Government Printing Office, 1965.

7. Greene, B. E., Strome, D. R., and Weikel, R. C., "Application of the Stiffness Method to the Analysis of Shell Structures," *ASME Paper* 61-AV-58, *Aviation Conference*, Los Angeles, Calif., March 12–16, 1961.

8. Clough, R. W. and Tocher, J. L., "Finite Element Stiffness Matrices for Analysis of Plate Bending," *Proc. Conf. on Matrix Methods in Struc. Mechs.*, AFFDL-TR-66-80, pp. 515–545, U. S. Government Printing Office, 1965.

9. Martin, H. C., "On the Derivation of Stiffness Matrices for the Analysis of Large Deflection and Stability Problems," *Proc. Conf. on Matrix Methods in Struct. Mechs.*, AFFDL-TR-66-80, pp. 697–715, U. S. Government Printing Office, 1965.

10. Martin, H. C., "Introduction to Matrix Methods of Structural Analysis," McGraw-Hill Book Co., New York, page 105, 1966.

11. Utku, S., "Computation of Stresses in Triangular Finite Elements," Technical Report 32–948, Jet Propulsion Laboratory, Pasadena, Calif., June 1966.

12. Timoshenko, S. and Woinowsky-Krieger, *Theory of Plates and Shells*, McGraw-Hill Book Co., New York.

13. Dong, S. B., Pister, K. S., and Taylor, R. L., "On the Theory of Laminated Anisotropic Shells and Plates," *J. Aerospace Sci.*, Vol. 29, No. 8, 1962.

References (contd)

14. Utku, S. and Melosh, R. J., "Behavior of Triangular Shell Element Stiffness Matrices Associated with Polyhedral Deflection Distributions," presented at *Fifth Aerospace Sciences Meeting*, New York, Jan. 23–26, 1967, AIAA Paper No. 67-114.

15. Martin, H. C., "On Plate and Shell Stability Analysis by the Direct Stiffness Method," presented at the *Thirteenth International Astronautical Congress*, Oct. 10–15, 1966, Madrid, Spain; to be published in Proceedings of the Congress.